Self-Assembled Nanostructures of Homopolymer and Diblock Copolymer Blends in a Selective Solvent

Guang-Kui Xu, Xi-Qiao Feng,* and Yue Li

Institute of Biomechanics and Medical Engineering, Department of Engineering Mechanics, Tsinghua University, Beijing 100084, China

Received: September 12, 2009; Revised Manuscript Received: November 22, 2009

Self-assembled nanostructures of amphiphilic block copolymers hold great promise for applications in nanomedicine. Blending polymers provides an effective way to produce multifunctional drug delivery vesicles at micro- and nanoscales. Here we investigate the self-assembly of homopolymer and diblock copolymer blends in a selective solvent by using the self-consistent field method. It is found that self-assembled nanostructures of different sizes and shapes (e.g., vesicles, circle- and line-like micelles, and their mixtures) can be obtained by varying the concentration and composition of the diblock copolymer. As the chain length or concentration of the homopolymer changes, morphological transitions may occur among the different nanostructures. On the basis of a number of simulations under various conditions, a phase diagram of aggregate morphologies is constructed with respect to the mixture ratio and the homopolymer chain length. The theoretical method presented here could be used to design novel nanomedicine carriers and to optimize their sizes and shapes for specific biomedical applications.

Introduction

Design and production of biocompatible and biodegradable nanoparticles have emerged as a highly promising area of research devoted toward developing novel drug delivery vehicles at micro- and nanoscales.[1,2] Among these nanomedicine carriers, liposomes and polymeric nanoparticles are two dominant classes for drug encapsulation, delivery, and release.[3] Liposomes have been widely used as drug delivery vehicles because they are biocompatible and capable of delivering various drug molecules.[4,5] Considerable attention has also been attracted to investigations of polymeric nanoparticles for targeted (cellular/tissue) drug delivery. Amphiphilic block copolymers can self-assemble into nanoparticles with a core−shell structure in aqueous solution, in which the hydrophobic core is capable of carrying highly insoluble drugs while the hydrophilic shell plays a stabilizing role.[6,7] Recently, Farokhzad et al. developed a protocol for the self-assembly of homopolymer and diblock copolymer, which possesses the advantages of both nanoparticles and liposomes.[8,9] By mixing the homopolymer and diblock copolymer in a certain mass ratio, a novel drug delivery vehicle has also been obtained to increase the loading drug.[10] Such self-assembled nanostructures contain a diblock monolayer surrounding a core made of the hydrophobic homopolymer.

The drug amount which can be loaded into each carrier and the particular drug release pattern rely not only on the hydrophilicity of the drug but also on the internal structure of the pharmaceutical carrier.[8−12] Controlling the shape and size of nanostructures is a fundamental and crucial issue in the design of nanosized drug delivery vehicles. Therefore, much effort has also been directed toward studying internal structures composed of amphiphilic block copolymers. The addition of homopolymer into amphiphilic copolymer micelles has been proved to be an efficient way to control the micelle size and even to modulate the aggregate morphology.[13,14] By putting a homopolymer into a solution of diblock copolymer, which can self-assemble into spherical micelles, the mean size of the micelles can be increased without distinct change in their morphology. In the case that a diblock copolymer self-assembles into rodlike micelles or vesicles, the addition of a homopolymer can also modulate their morphologies.[13,14] Besides the stoichiometry of polymers, the composition of copolymers is another important factor that influences not only the particle size[12,15−19] but also the drug encapsulation efficiency, drug release rate, and cellular uptake.[15−19] For amphiphilic block copolymer micelles, in general, a higher fraction of hydrophobic chain will raise the micelle size.[15−17,20] In addition, for biomedical applications of nanostructured polymer materials, a crucial issue is to correlate their synthesis process, structure, and properties.[21,22] In particular, exploring the conditions that yield self-assembled polymer nanostructures with specific physical and chemical properties has attracted considerable attention.[22]

As a mesoscopic polymer theory, the self-consistent field theory (SCFT) has its origin from the field theoretical approach of Edwards[23] and was explicitly adopted to deal with block copolymer structures by Helfand.[24] In this theory, the local monomer densities are conjugated to the chemical potential fields, and then the free energy of the system is determined as a function of these variables. SCFT has proven to be a powerful tool to explore the self-assembly and other thermodynamic processes of block copolymers, based on the mean field representation of internal energy and entropy.[25−28] It has also been extended to predict the nanostructures of polymer-grafted nanoparticles,[29] which have potential applications in the design and synthesis of hierarchical materials.[30−32] In addition, SCFT allows us to investigate the aggregate morphology of amphiphilic block copolymers and their blends in a dilute solution.[33−39] These studies show that the aggregate morphologies depend on the initial density fluctuation, interaction parameter, mixture ratio, and polydispersity.[33−39] Recently, we employed SCFT to study the self-assembly behavior of diblock copolymers surrounding a hydrophobic nanoparticle in aqueous

* Corresponding author. Tel.: +86-10-6277 2934. Fax: +86-10-6278 1824. E-mail: fengxq@tsinghua.edu.cn.

10.1021/jp908823h © 2010 American Chemical Society
Published on Web 01/05/2010

solution.[40] It is demonstrated that under different conditions of particle surface treatment diblock copolymers can self-assemble into monolayered or bilayered structures encapsulating the nanoparticle.

To date, however, there is a lack of theoretical investigation on the self-assembly of diblock copolymer and homopolymer blends in a selective solvent. In recognition of its significance in the nanomedicine field, this problem is studied here by using a two-dimensional SCFT-based numerical method. It is found that various nanostructures can form in the solution, e.g., vesicles and circle- and line-like micelles. Especially, we examine the dependence of the shape and size of the self-assembled nanostructures on such key factors as the stoichiometric ratio, the homopolymer chain length, and the composition of copolymers. These factors play significant roles in the self-assembly process and can be easily controlled in experiments to produce nanostructures with designed size and shape.

Theoretical Model and Computational Method

Consider a system of volume V, containing a diblock copolymer, a homopolymer, and a solvent. All polymer chains are modeled as flexible Gaussian chains. The hydrophobic homopolymer is used to encapsulate drugs that are poorly soluble in solution. Each homopolymer chain is composed of N_H segments (H), while each diblock copolymer chain consists of N_D total segments, including N_A hydrophobic (A) and N_B hydrophilic segments (B), i.e., $N_D = N_A + N_B$. The volume fraction of the A segments per diblock copolymer chain is denoted as $f = N_A/N_D$. For simplicity, assume that all the H, A, and B segments and solvent molecules have the same volume ρ_0^{-1} and statistical length a. The volume fractions of the diblock copolymer and homopolymer in the solution are φ_D and φ_H, respectively, and that of the solvent is $\varphi_S = 1 - \varphi_D - \varphi_H$ because the mixture is assumed to be incompressible.

In the SCFT method, the pair interactions between different components are determined by a set of effective chemical potential fields $W_I(\mathbf{r})$ (I = A, B, H, and S), which denote the intensity of the mean field felt by the species I at position $\mathbf{r}$. In the canonical ensemble, the dimensionless free energy of the system is given by

$$\frac{N_D F}{\rho_0 k_B T V} = -\varphi_D \ln\left(\frac{Q_D}{V\phi_D}\right) - \frac{\varphi_H}{\alpha}\ln\left(\frac{Q_H}{V\varphi_H}\right) - N_D\varphi_S \ln\left(\frac{Q_S}{V\varphi_S}\right) - \frac{1}{V}\int d\mathbf{r}[W_A\phi_A + W_B\phi_B + W_H\phi_H + W_S\phi_S + \xi(1 - \phi_A - \phi_B - \phi_H - \phi_S)] + \frac{1}{V}\int d\mathbf{r}(N_D\chi_{AB}\phi_A\phi_B + N_D\chi_{BS}\phi_B\phi_S + N_D\chi_{AS}\phi_A\phi_S + N_D\chi_{AH}\phi_A\phi_H + N_D\chi_{BH}\phi_B\phi_H + N_D\chi_{HS}\phi_H\phi_S) \quad (1)$$

where k_B is the Boltzmann constant; T is the temperature; χ_{IJ} is the Flory−Huggins interaction parameter betweens species I and J; ξ is a Lagrange multiplier enhancing the incompressible condition; $\phi_I(\mathbf{r})$ denotes the local volume fraction of species I at position $\mathbf{r}$; and $\alpha = N_H/N_D$ is the volume ratio between a homopolymer chain and a diblock copolymer chain. $Q_D = \int d\mathbf{r}\, q_D(\mathbf{r},1)$ is the partition function of a single diblock copolymer chain under the fields $W_A(\mathbf{r})$ and $W_B(\mathbf{r})$; $Q_H = \int d\mathbf{r}\, q_H(\mathbf{r},\alpha)$ is the partition function of a single homopolymer chain subject to the field $W_H(\mathbf{r})$; and $Q_S = \int d\mathbf{r} \exp[-W_S(\mathbf{r})/N_D]$ is the partition function of a solvent molecule in the field $W_S(\mathbf{r})$.

For a diblock copolymer chain, the contour variable s increases continuously from $s = 0$ at the beginning of the A-blocks to $s = 1$ at the end of the B-blocks. For a homopolymer chain, s runs from 0 to α. The spatial coordinate $\mathbf{r}$ is normalized by the diblock radius of gyration, $R_g = a\sqrt{N_D}/6$. The propagator $q_D(\mathbf{r},s)$ represents the probability of finding segments s of the diblock copolymer at position $\mathbf{r}$, which satisfies the modified diffusion equation

$$\frac{\partial q_D(\mathbf{r},s)}{\partial s} = \nabla^2 q_D(\mathbf{r},s) - W_I(\mathbf{r}) q_D(\mathbf{r},s) \quad (2)$$

$$W_I(\mathbf{r}) = \begin{cases} W_A(\mathbf{r}), & 0 < s < f \\ W_B(\mathbf{r}), & f < s < 1 \end{cases} \quad (3)$$

subject to the initial condition $q_D(\mathbf{r},0) = 1$. The complementary propagator $q_D^+(\mathbf{r},s)$ satisfies an equation similar to eq 2 except that its right-hand side is multiplied by -1 and the initial condition becomes $q_D^+(\mathbf{r},1) = 1$. The homopolymer chain propagator $q_H(\mathbf{r},s)$ satisfies

$$\frac{\partial q_H(\mathbf{r},s)}{\partial s} = \nabla^2 q_H(\mathbf{r},s) - W_H(\mathbf{r}) q_H(\mathbf{r},s) \quad (4)$$

with the initial condition being $q_H(\mathbf{r},0) = 1$.

The local volume fractions of the A, B, H, and solvent components are calculated, respectively, by

$$\phi_A(\mathbf{r}) = \frac{\varphi_D V}{Q_D}\int_0^f ds\, q_D(\mathbf{r},s) q_D^+(\mathbf{r},s) \quad (5)$$

$$\phi_B(\mathbf{r}) = \frac{\varphi_D V}{Q_D}\int_f^1 ds\, q_D(\mathbf{r},s) q_D^+(\mathbf{r},s) \quad (6)$$

$$\phi_H(\mathbf{r}) = \frac{\varphi_H V}{Q_H \alpha}\int_0^\alpha ds\, q_H(\mathbf{r},s) q_H(\mathbf{r},\alpha - s) \quad (7)$$

$$\phi_S(\mathbf{r}) = \frac{\varphi_S V}{Q_S}\exp[-W_S(\mathbf{r})/N_D] \quad (8)$$

By minimizing the free energy F with respect to $\phi_I(\mathbf{r})$ and $\xi(\mathbf{r})$, i.e., $\partial F/\partial\phi_I = \partial F/\partial\xi = 0$, one has the following equations

$$W_A(\mathbf{r}) = N_D\chi_{AB}\phi_B(\mathbf{r}) + N_D\chi_{AH}\phi_H(\mathbf{r}) + N_D\chi_{AS}\phi_S(\mathbf{r}) + \xi(\mathbf{r}) \quad (9)$$

$$W_B(\mathbf{r}) = N_D\chi_{AB}\phi_A(\mathbf{r}) + N_D\chi_{BH}\phi_H(\mathbf{r}) + N_D\chi_{BS}\phi_S(\mathbf{r}) + \xi(\mathbf{r}) \quad (10)$$

$$W_H(\mathbf{r}) = N_D\chi_{AH}\phi_A(\mathbf{r}) + N_D\chi_{BH}\phi_B(\mathbf{r}) + N_D\chi_{HS}\phi_S(\mathbf{r}) + \xi(\mathbf{r}) \quad (11)$$

$$W_S(\mathbf{r}) = N_D\chi_{AS}\phi_A(\mathbf{r}) + N_D\chi_{BS}\phi_B(\mathbf{r}) + N_D\chi_{HS}\phi_H(\mathbf{r}) + \xi(\mathbf{r}) \quad (12)$$

$$\phi_A(\mathbf{r}) + \phi_B(\mathbf{r}) + \phi_H(\mathbf{r}) + \phi_S(\mathbf{r}) = 1 \quad (13)$$

Equations 5−13 form a closed set of equations that can be solved self-consistently in real space. To obtain the equilibrium nanostructure, we solve these equations by using the combina-

torial screening technique of Drolet and Fredrickson[27,28] implemented with a highly stable and accurate numerical algorithm.[41,42] The initial values of the density fields $\phi_I(\mathbf{r})$ satisfy the Gaussian distributions[33]

$$\langle \phi_I(\mathbf{r}) - \varphi_I \rangle = 0 \tag{14}$$

$$\langle (\phi_I(\mathbf{r}) - \varphi_I)(\phi_J(\mathbf{r'}) - \varphi_J) \rangle = \beta \varphi_I \varphi_J \delta_{IJ} \delta(\mathbf{r} - \mathbf{r'}) \tag{15}$$

where β characterizes the intensity of initial density fluctuation and φ_I represents the average volume fraction of species I. All the simulations are performed in a two-dimensional 128 × 128 square lattice with periodic boundary conditions. The contour's step size is set to be 0.01. Previous studies showed that the density fluctuation amplitude at the initial state, represented by the parameter β, affects the self-assembly of polymers in dilute solution.[33] To examine the influence of initial density fluctuations, therefore, we will compare the morphologies of self-assembled nanostructures under two representative values of β (10^{-1} and 10^{-6}). When the effects of other factors are under study, we will set β to be constant, as suggested by refs 34, 39, and 43. Besides, the chain length should also be in a moderate range to decrease the fluctuation effects. The system is thought to have reached equilibrium when the relative difference between the free energies of the system at two neighboring iteration steps has been smaller than 0.001% and the incompressibility condition has been achieved. Furthermore, in each situation, we repeat the simulations many times using different random numbers to ensure that the obtained structures are not accidental. More details on the numerical implementation of SCFT can be found in the literature.[27,28,41,42]

Results and Discussions

We study the self-assembly of a homopolymer (H) and a diblock copolymer (AB) mixed in a selective solvent. The normalized length of the simulation box is taken as $L = 32$, and the grid size $\Delta x = 0.25$. The total volume fraction of polymers is fixed at $\varphi_D + \varphi_H = 0.1$ to ensure that the polymer solution is dilute. Assume that the B-blocks are hydrophilic while the A- and H-blocks are hydrophobic and poorly soluble in the solution. In this case, the solvent has a preferential interaction to the B-blocks, and the corresponding interaction parameter is set as $\chi_{BS} = -0.25$. The interaction parameters of the A- and H-blocks with the solvent are assumed to be $\chi_{AS} = \chi_{HS} = 1.25$. In addition, we adopt the following representative values for the interactions among different components: $\chi_{AH} = 0.025$ and $\chi_{AB} = \chi_{BH} = 1.0$. Unless stated otherwise, the chain lengths of the homopolymer and diblock copolymer are fixed as $N_H = N_D = 20$, i.e., $\alpha = 1$. The volume fraction of A-blocks in each diblock copolymer chain, f, is taken to be 0.85. In this paper, our attention is focused on the effects of such factors as the stoichiometric ratio, the homopolymer chain length, and the composition of the diblock copolymer because these factors play significant roles in the self-assembly process and can be easily controlled in experiments to create various nanostructures.

1. Effect of the Stoichiometric Ratio. We first compare the self-assembled structures of the diblock copolymer in the absence of homopolymer under different values of the initial density fluctuation parameter β. It is found that the diblock copolymer can assemble into circle-like micelles under big initial fluctuation (e.g., $\beta = 10^{-1}$) or vesicles under small initial fluctuation (e.g., $\beta = 10^{-6}$), as shown in Figure 1. This result

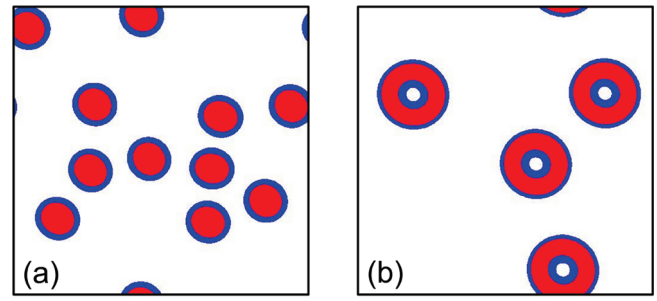

Figure 1. Aggregate morphologies of the diblock copolymer in a dilute solution under different initial density fluctuations: (a) circle-like micelles under $\beta = 10^{-1}$ and (b) vesicles under $\beta = 10^{-6}$. The red, blue, and white colors stand for A-blocks, B-blocks, and solvent molecules, respectively.

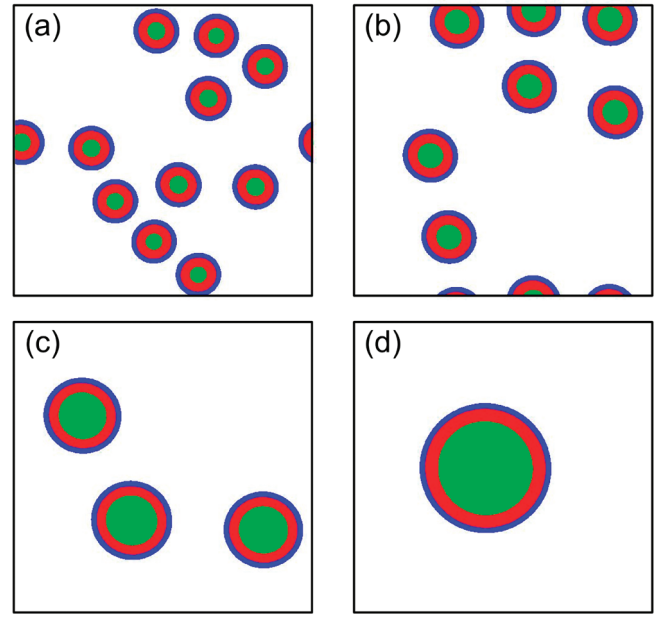

Figure 2. Self-assembled core−shell−corona nanostructures by the homopolymer and diblock copolymer blend in a dilute solution with an increase in the homopolymer concentration φ_H: (a) $\varphi_H = 0.01$, (b) $\varphi_H = 0.03$, (c) $\varphi_H = 0.052$, and (d) $\varphi_H = 0.08$. The red, blue, green, and white colors represent A-, B-, and H-blocks and solvent molecules, respectively. Here we take $\beta = 10^{-1}$.

is in agreement with that of He et al.[33] In what follows, therefore, we will examine the effect of the mixture ratio of homopolymer and diblock copolymer on their self-assembly behavior under these two representative situations of initial fluctuation. We will observe the evolution of the aggregate morphology with increasing the homopolymer content in the solution.

In the case of $\beta = 10^{-1}$, the diblock copolymer self-assembles into circle-like micelles in the absence of homopolymer (Figure 1a). Under four representative homopolymer concentrations, $\varphi_H = 0.01$, 0.03, 0.052, and 0.08, the assembled nanostructures of the homopolymer and diblock copolymer are shown in Figure 2a−d, respectively. It is seen that a core−shell−corona structure forms, in which the hydrophobic H- and A-blocks form the core (green) and the shell (red), respectively, and the corona (blue) is made of hydrophilic B-blocks. With the increase of φ_H, the mean size of the obtained micelles increases, but their morphologies do not have evident change.

To reveal the structure more clearly, the density profiles of the four components along the diameter direction of a core−shell−corona structure are plotted in Figure 3a, where ϕ_A, ϕ_B, ϕ_H, and ϕ_S denote the density of A-, B-, and H-blocks

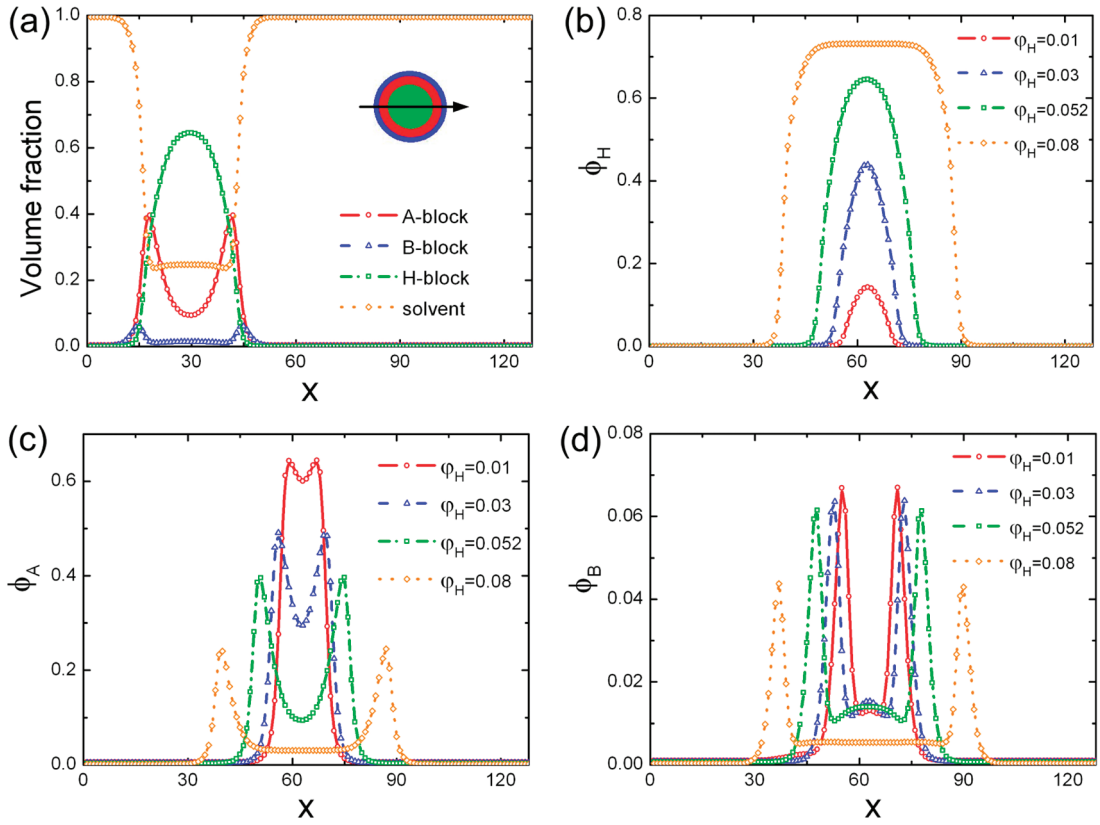

Figure 3. (a) Density profiles of A- (red), B- (blue), and H-blocks (green) and solvent molecules (orange) along the diameter direction of a micelle chosen from Figure 2c. The density profiles for four representative micelles selected from Figure 2a−d are compared: (b) φ_H, (c) φ_A, and (d) φ_B.

and solvent molecules per unit area. For comparison, the centers of the four micelles have been placed at the same position. The hydrophobic H-blocks have a high density only in the central region of the micelle, indicating that the homopolymer is concentrated in the interior of the shell. Both the A- and B-block density profiles show a bimodal feature. The hydrophobic component of the diblock copolymer points to the core, while the hydrophilic component points outward. The formation of this structure is attributed to the preferential interaction between the H- and A-blocks and that between the solvent and B-blocks. The biodegradable hydrophobic core can carry insoluble drugs, while the hydrophilic corona enhances the stability of the vehicles in solution. Such a self-assembled structure has been observed in recent experiments.[8,9,12] It is also in agreement with our previous simulation result that lipid molecules can form a monolayer surrounding a hydrophobic nanoparticle.[40]

As can be seen from the corresponding density profiles in Figure 3b−d, a larger micelle can be designed by increasing the volume fraction of the homopolymer. Because the H-blocks are repulsive to the B-blocks and solvent molecules, additional homopolymer molecules are forced into the core to reduce the free energy of the system, leading to the expansion of the micelle. The increasing trend of the mean micelle size with the increase in the homopolymer content is consistent with recent relevant experimental observations.[10,12,13]

Furthermore, with the increase of φ_H, the peak value of the H-block density ϕ_H increases (Figure 3b), whereas those of A- and B-block density profiles decrease (Figure 3c,d). This can be easily understood by considering the relative change of the number of homopolymer and diblock copolymer molecules under the condition that their total number is constant in all the simulations. Thus, for a larger value of φ_H, the shell (A-blocks) and corona (B-blocks) are relatively incompact because of the reduced number of A or B segments, while the core consisting of H-blocks becomes denser.

Under small initial fluctuation (e.g., $\beta = 10^{-6}$), the diblock copolymer assembles into vesicles in the solution without a homopolymer (Figure 1b). By adding the homopolymer, the mixtures self-assemble into several different forms of nanostructures, as shown in Figure 4. Under a low volume fraction of homopolymer (e.g., $\varphi_H = 0.01$), layered vesicles are obtained (Figure 4a), each of which contains two layers of the diblock copolymer and a sandwiched homopolymer layer. In the outer layer of a vesicle, the B-blocks of the diblock copolymer molecules face outward due to their favorable attraction to the solvent molecules, while in the middle layer, the A-blocks of the diblock copolymer point inward. The density profiles of all the four species in a self-assembled vesicle are plotted in Figure 5a, which also clearly illustrates the layered structure consisting of H-, A-, and B-blocks from the interior to the exterior.

As φ_H increases, our simulations reveal an interesting transition of the morphology of the self-assembled nanostructures. In the case of $\varphi_H = 0.02$, vesicles (V), line-like, and circle-like micelles (V+L+C) coexist in the solution, as shown in Figure 4b. When $\varphi_H = 0.03$, line-like and circle-like micelles (L+C) are obtained, but few vesicles are observable (Figure 4c). For a higher homopolymer concentration (e.g., $\varphi_H = 0.04$), only circle-like micelles (C) are assembled (Figure 4d). With the increase in φ_H, as aforementioned, the concentration of diblock copolymer φ_D decreases because of the fixed value of $\varphi_H + \varphi_D = 0.1$. The number of copolymer molecules in a vesicle is about two times than that in a circle-like micelle of the same size. Therefore, when the total number of diblock copolymer molecules in the solution is insufficient to constitute

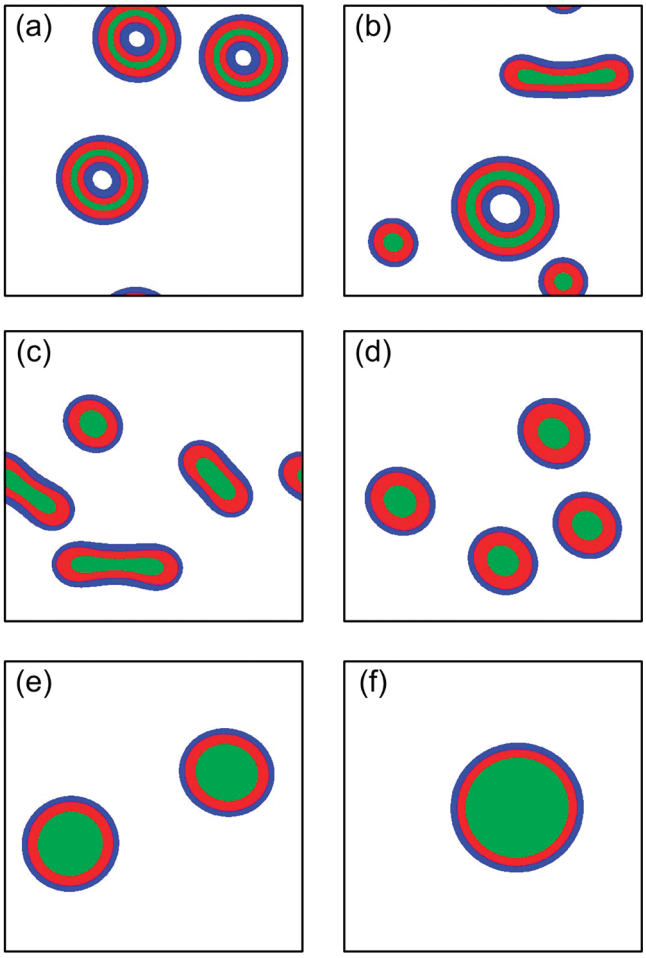

Figure 4. Self-assembled nanostructures by the homopolymer and diblock copolymer blend in a dilute solution with an increase in the homopolymer concentration φ_H: (a) $\varphi_H = 0.01$, (b) $\varphi_H = 0.02$, (c) $\varphi_H = 0.03$, (d) $\varphi_H = 0.04$, (e) $\varphi_H = 0.057$, and (f) $\varphi_H = 0.075$. The red, blue, green, and white colors represent A-blocks, B-blocks, H-blocks, and solvent molecules, respectively. In this figure, we take $\beta = 10^{-6}$.

vesicles enwrapping the added homopolymer, they will tend to form micelles. As a consequence, the morphological transitions in the order of V, (V+L+C), (L+C), and C happen with increasing φ_H. When adding a homopolymer into a diblock copolymer solution, Zhang and Eisenberg experimentally observed a morphology transition of self-assembled structures from vesicles or rod-like micelles to spherical micelles.[13] The line-like and circle-like micelles in the two-dimensional SCFT simulations correspond, respectively, to the rod-like and spherical micelles in their experiments. Therefore, the prominent features of morphological transitions found in our numerical simulations are basically agreeable with their observations, and the theoretical prediction of the transition progress is more informative.

As φ_H increases further, only circle-like micelles will be obtained without distinct change of morphology, but their mean diameter becomes larger and larger (Figure 4d−f). The density profiles for four representative micelles selected from Figure 4d−f are compared in Figure 5b−d, respectively. The distribution of H-blocks has a peak value in the central region of the micelle, whereas A- and B-blocks show a bimodal feature. The changing trends of their density profiles and their underlying physical mechanisms as well are basically the same as the case under a big initial fluctuation in Figure 3b−d.

2. Effect of the Composition of the Diblock Copolymer. In this subsection, we address the effect of the composition of diblock copolymer on the assembled nanostructures under a small value of initial density fluctuation amplitude ($\beta = 10^{-6}$). The composition of diblock copolymer f is varied in the range from 0.8 to 0.92 under a fixed chain length of diblock copolymer, $N_D = 25$. A larger f indicates a longer hydrophobic component (or more A-blocks). The chain length and the volume fraction of homopolymer are set to be $N_H = 16$ and $\varphi_H = 0.05$, respectively. For several representative values of f, the aggregate morphologies are compared in Figure 6. In all these situations, the mixtures self-assemble into concentric core−shell−corona structures, in which the homopolymer forms the core enwrapped by the diblock copolymer. As f increases, the mean size of micelles increases, whereas their number decreases. The dependence of the mean micelle size can be explained from the viewpoint of conformational entropy. For a large value of f, each diblock copolymer molecule contains more hydrophobic segments (A). They tend to enlarge the mean size and reduce the total number of micelles, which corresponds to higher conformational entropy. For amphiphilic block copolymers, the conclusion that a longer hydrophobic block length results in an increase in the assembled micelle size is in accord with relevant experiments.[15–17]

3. Effect of the Chain Length of Homopolymer Molecules. Then, we study the dependence of self-assembled structures on the homopolymer chain length N_H under a specified volume fraction of homopolymer, $\varphi_H = 0.028$. For the diblock copolymer, the chain length is fixed at $N_D = 20$, and the composition of A-blocks is set as $f = 0.85$. Figure 7 shows the obtained nanostructures under various values of N_H. For a short chain length of homopolymer (e.g., $N_H = 6$), the two polymers assemble into layered vesicles consisting of H-, A-, and B-blocks in their interior, middle, and exterior parts, respectively. Increasing the homopolymer chain length leads to the morphological transformation of aggregates in the order of V→(V+L+C)→(L+C)→C. As N_H increases, the homopolymer is more favorable to form a core, rendering a smaller contact area with other species and a reduction of the internal energy. Therefore, it is the minimization of the free energy of the system that directs the morphology transition. Zhang et al. recently demonstrated that the aggregate morphology of diblock copolymer and nanoparticle blends undergoes a transition from vesicles to coexistence of tubular and circle-like micelles as the particle radius increases.[43] Varying the homopolymer chain length in our system is somewhat similar to changing the particle radius in theirs because both the homopolymer and particle constitute the core of the aggregates. Therefore, the SCFT-based numerical method presented in this study can well predict the complicated structural and morphological transitions of assembled nanostructures of polymer blends in solution.

4. Phase Diagram of Self-Assembled Nanostructures. To reveal the dependence of the self-assembled nanostructures upon the concentration and chain length of homopolymer, a phase diagram of aggregate morphology is given in Figure 8 based on a sufficient number of simulations. Corresponding to distinctly different structures and morphologies of the aggregates, the diagram is divided into four regions, marked by V, (V+L+C), (L+C), and C, respectively. Such a phase diagram allows us to predict specific nanostructures formed by the homopolymer and diblock polymer blends under given conditions as well as morphological transitions with varying the blending conditions.

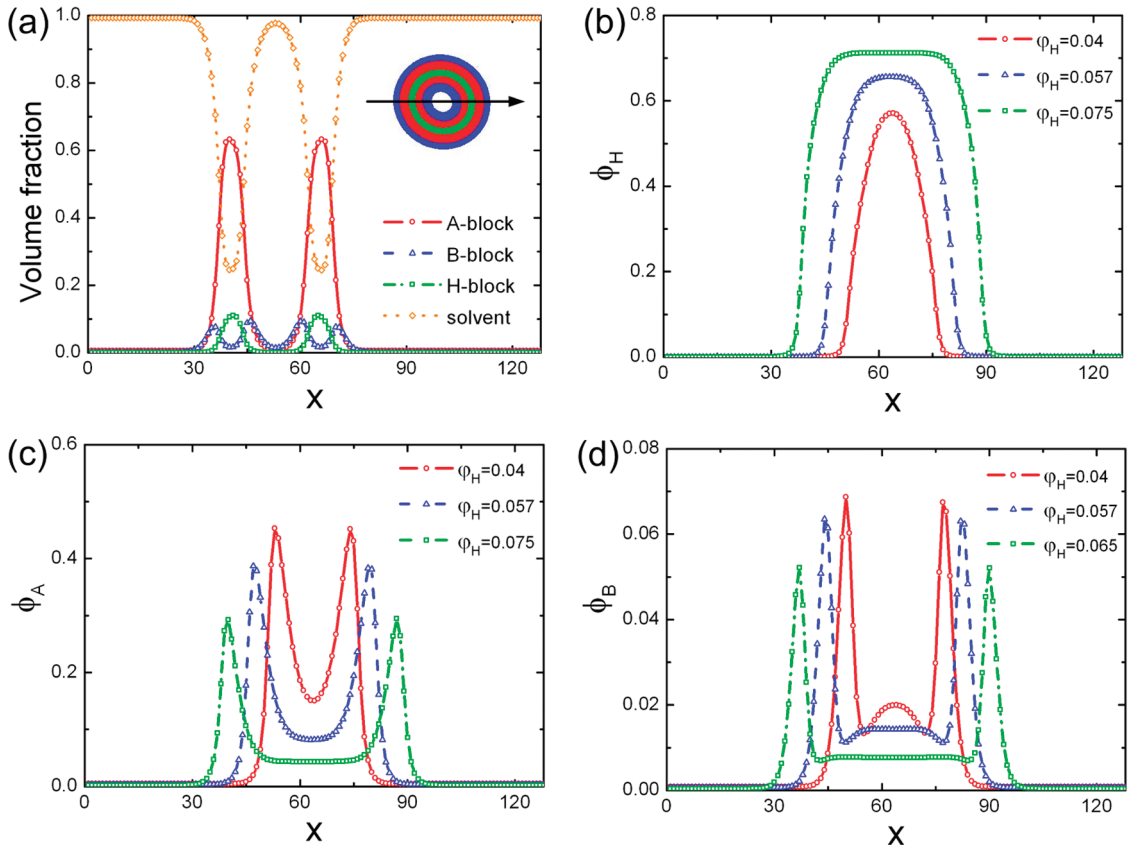

Figure 5. (a) Density profiles of A-blocks (red), B-blocks (blue), H-blocks (green), and solvent molecules (orange) along the diameter direction of a vesicle chosen from Figure 4a. The density profiles for four representative micelles selected from Figure 4d−f are compared: (b) φ_H, (c) φ_A, and (d) φ_B.

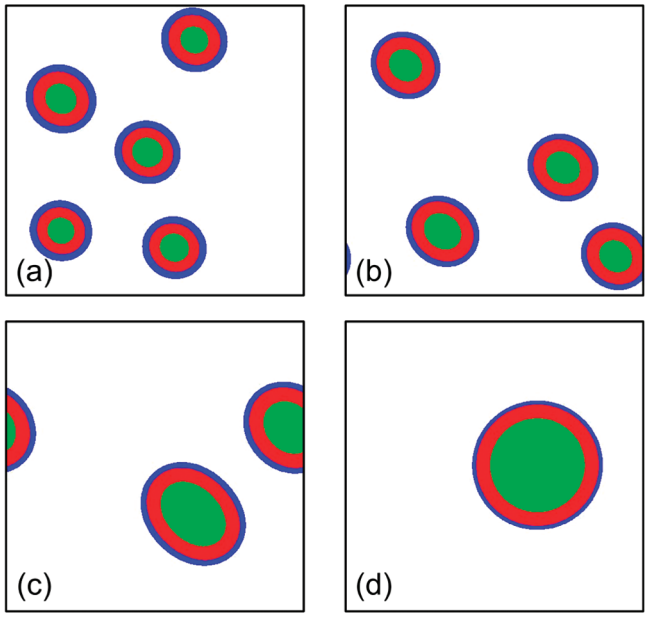

Figure 6. Aggregate morphologies self-assembled by the homopolymer and diblock copolymer blend in a dilute solution under several representative values of diblock copolymer composition: (a) $f = 0.8$, (b) $f = 0.84$, (c) $f = 0.88$, and (d) $f = 0.92$. The red, blue, green, and white colors represent A-blocks, B-blocks, H-blocks, and solvent molecules, respectively. Here we take $\varphi_H = 0.05$.

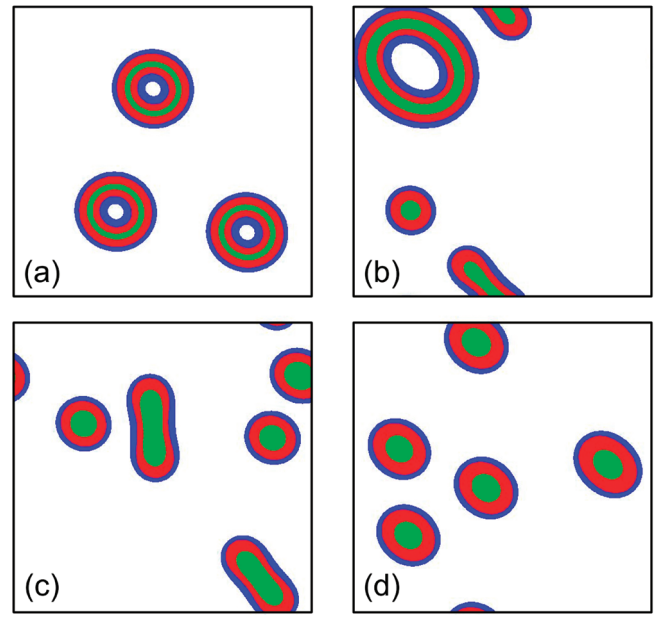

Figure 7. Aggregate morphologies self-assembled by the homopolymer and diblock copolymer blend in a dilute solution under several representative values of homopolymer chain length: (a) $N_H = 6$, (b) $N_H = 15$, (c) $N_H = 24$, and (d) $N_H = 32$. The red, blue, green, and white colors represent A-blocks, B-blocks, H-blocks, and solvent molecules, respectively. Here we take $\varphi_H = 0.028$.

Conclusions

We have presented a SCFT method to investigate the self-assembled nanostructures of hydrophobic homopolymer and amphiphilic diblock copolymer blends in a selective solvent. It is found that the assembled structures depend on such factors as the mixture ratio of two polymers, the homopolymer chain length, and the diblock copolymer composition. Under the condition of big initial fluctuation, the diblock copolymer in a

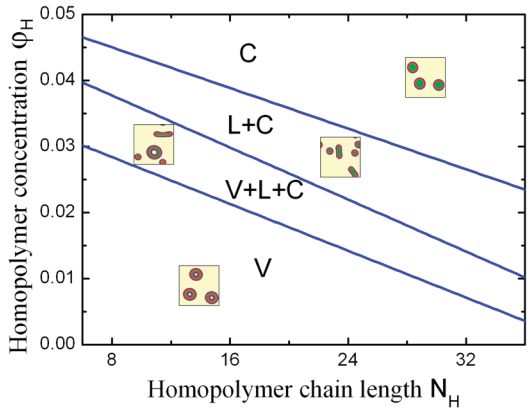

Figure 8. Phase diagram illustrating the dependence of self-assembled nanostructures on the concentration φ_H and chain length N_H of homopolymer. The diagram is divided into four regions: V, (V+L+C), (L+C), and C. The notations V, L, and C stand for vesicles, line-like, and circle-like micelles, respectively.

dilute solution forms circle-like micelles, and adding the homopolymer enlarges the mean size of the micelles but does not change their morphology. Under small initial fluctuation, the diblock copolymer self-assembles into vesicles, and a morphology transition in the order of V→(V+L+C)→(L+C)→C can be achieved either by adding the homopolymer or increasing the homopolymer chain length. Additionally, the mean size of micelles increases with elongating the hydrophobic composition fraction of diblock copolymer molecules. Our simulation results demonstrate that the shape and size of self-assembled structures can be tuned by varying the polymer volume fractions and chain lengths, which can be easily tailored in experiments. Different structures of drug delivery vehicles exhibit different ability in drug encapsulation efficiency, drug release rate, and cellular uptake efficiency.[8–12,15–19] This study is helpful for optimal design of novel drug delivery vehicles with controlled shape and size, which have promising applications in the field of nanomedicine.

Acknowledgment. The support from the National Natural Science Foundation of China (Grants Nos. 10972121, 10732050, and 10525210) and the 973 program of MOST (2010CB631005) is acknowledged.

References and Notes

(1) Ferrari, M. *Nat. Rev. Cancer* **2005**, *5*, 161–171.
(2) Farokhzad, O. C.; Langer, R. *Adv. Drug Delivery Rev.* **2006**, *58*, 1456–1459.
(3) Wagner, V.; Dullaart, A.; Bock, A. K.; Zweck, A. *Nat. Biotechnol.* **2006**, *24*, 1211–1217.
(4) Torchilin, V. P. *Nat. Rev. Drug Discovery* **2005**, *4*, 145–160.
(5) Zhang, L.; Granick, S. *Nano Lett.* **2006**, *6*, 694–698.
(6) Otsuka, H.; Nagasaki, Y.; Kataoka, K. *Adv. Drug Delivery Rev.* **2003**, *55*, 403–419.
(7) Ai, H.; Flask, C.; Weinberg, B.; Shuai, X.; Pagel, M. D.; Farrell, D.; Duerk, J.; Gao, J. *Adv. Mater.* **2005**, *17*, 1949–1952.
(8) Zhang, L.; Chan, J. M.; Gu, F. X.; Rhee, J.-W.; Wang, A. Z.; Radovic-Moreno, A. F.; Alexis, F.; Langer, R.; Farokhzad, O. C. *ACS Nano* **2008**, *2*, 1696–1702.
(9) Chan, J. M.; Zhang, L.; Yuet, K. P.; Liao, G.; Rhee, J.-W.; Langer, R.; Farokhzad, O. C. *Biomaterials* **2009**, *30*, 1627–1634.
(10) Layre, A.; Couvereur, P.; Chacun, H.; Richard, J.; Passirani, C.; Requier, D.; Benoit, J. P.; Gref, R. *J. Controlled Release* **2006**, *111*, 271–280.
(11) Shenoy, D.; Little, S.; Langer, R.; Amiji, M. *Mol. Pharmacol.* **2005**, *2*, 357–366.
(12) Cho, E. C.; Cho, K.; Ahn, J. K.; Kim, J.; Chang, I.-S. *Biomacromolecules* **2006**, *7*, 1679–1685.
(13) Zhang, L.; Eisenberg, A. *J. Am. Chem. Soc.* **1996**, *118*, 3168–3181.
(14) Choucair, A.; Eisenberg, A. *Eur. Phys. J. E* **2003**, *10*, 37–44.
(15) Avgoustakis, K.; Beletsi, A.; Panagi, Z.; Klepetsanis, P.; Livaniou, E.; Evangelatos, G.; Ithakissios, D. S. *Int. J. Pharm.* **2003**, *259*, 115–127.
(16) Hu, Y.; Xie, J.; Tong, Y. W.; Wang, C.-H. *J. Controlled Release* **2007**, *118*, 7–17.
(17) Lin, W.-J.; Juang, L.-W.; Lin, C.-C. *Pharm. Res.* **2003**, *20*, 668–673.
(18) Gu, F.; Zhang, L.; Teply, B. A.; Mann, N.; Wang, A.; Fadovic-Moreno, A. F.; Langer, R.; Farokhzad, O. C. *Proc. Natl. Acad. Sci. U.S.A.* **2008**, *105*, 2586–2591.
(19) Mosqueira, V. C. F.; Legrand, P.; Gulik, A.; Bourdon, O.; Gref, R.; Labarre, D.; Barratt, G. *Biomaterials* **2001**, *22*, 2967–2979.
(20) Mosqueira, V. C. F.; Legrand, P.; Morgat, J.-L.; Vert, M.; Mysiakine, E.; Gref, R.; Devissaguet, J.-P.; Barratt, G. *Pharm. Res.* **2001**, *18*, 1411–1419.
(21) Buehler, M. J.; Ackbarow, T. *Mater. Today* **2007**, *10*, 46–58.
(22) Buehler, M. J.; Yung, Y. C. *Nat. Mater.* **2009**, *8*, 175–188.
(23) Edwards, S. F. *Proc. Phys. Soc.* **1965**, *85*, 613–624.
(24) Helfand, E. *J. Chem. Phys.* **1975**, *62*, 999–1005.
(25) Matsen, M. W.; Schick, M. *Phys. Rev. Lett.* **1994**, *72*, 2660–2663.
(26) Matsen, M. W. *Soft Matter*; Gompper, G., Schick, M., Eds.; Wiley-VCH: Weinheim, Germany, 2006; Vol. 1.
(27) Drolet, F.; Fredrickson, G. H. *Phys. Rev. Lett.* **1999**, *83*, 4317–4320.
(28) Drolet, F.; Fredrickson, G. H. *Macromolecules* **2001**, *34*, 5317–5324.
(29) Reister, E.; Fredrickson, G. H. *J. Chem. Phys.* **2005**, *123*, 214903.
(30) Zhang, Z.; Horsch, M. A.; Lamm, M. H.; Glotzer, S. C. *Nano. Lett.* **2003**, *3*, 1341–1346.
(31) Böker, A.; Lin, Y.; Chiapperini, K.; Horowitz, R.; Thompson, M.; Carreon, V.; Xu, T.; Abetz, C.; Skaff, H.; Dinsmore, A. D.; Emrick, T.; Russell, T. P. *Nat. Mater.* **2004**, *3*, 302–306.
(32) Zhang, J.; Wang, Z.-L.; Liu, J.; Chen, S.; Liu, G.-Y. *Self-Assembled Nanostructures*;Kluwer Academic/Plenum Publishers: New York, 2003.
(33) He, X.; Liang, H.; Huang, L.; Pan, C. *J. Phys. Chem. B* **2004**, *108*, 1731–1735.
(34) Jiang, Y.; Chen, T.; Ye, F.; Liang, H.; Shi, A.-C. *Macromolecules* **2005**, *38*, 6710–6717.
(35) Wang, R.; Tang, P.; Qiu, F.; Yang, Y. *J. Phys. Chem. B* **2005**, *109*, 17120–17127.
(36) Wang, R.; Jiang, Z.; Chen, Y.-L.; Xue, G. *J. Phys. Chem. B* **2006**, *110*, 22726–22731.
(37) Li, X.; Tang, P.; Qiu, F.; Zhang, H.; Yang, Y. *J. Phys. Chem. B* **2006**, *110*, 2024–2030.
(38) Ma, J. W.; Li, X.; Tang, P.; Yang, Y. *J. Phys. Chem. B* **2007**, *111*, 1552–1558.
(39) Zhuang, Y.; Lin, J.; Wang, L.; Zhang, L. *J. Phys. Chem. B* **2009**, *113*, 1906–1913.
(40) Xu, G.-K.; Li, Y.; Li, B.; Feng, X.-Q.; Gao, H. *Soft Matter* **2009**, *5*, 3977–3983.
(41) Tzeremes, G.; Rasmussen, K. Ø.; Lookman, T.; Saxena, A. *Phys. Rev. E* **2002**, *65*, 041806.
(42) Sides, S. W.; Fredrickson, G. H. *Polymer* **2003**, *44*, 5859–5866.
(43) Zhang, L.; Lin, J.; Lin, S. *Macromolecules* **2007**, *40*, 5582–5592.

JP908823H